INPUT IMPEDANCE CALCULATION OF DIPOLE ANTENNA USING FDTD METHOD

Wenhua Yu,[1] Xiaoling Yang,[1] Yongjun Liu,[1] Raj Mittra,[1] Yongquan Lu,[2] Pai Wang,[2] Qing Che,[2] and Rui Lu[2]
[1] Electromagnetic Communication Lab, The Pennsylvania State University, PA 16801; Corresponding author: wxy6@psu.edu
[2] High Performance Center, Communication University of China, Beijing 100024, China

Received 28 December 2007

ABSTRACT: *Since the input impedance of half wavelength dipole antenna is well known, therefore, a dipole antenna is frequently used to validate the computational electromagnetic method. Though its structure is relatively simple, it is not a simple problem for the most computational electromagnetic methods. In this article, we investigate the input impedance of half wavelength dipole antenna using the FDTD method. Numerical experiments have demonstrated that the FDTD method can be used to accurately calculate its input impedance using uniform mesh, nonuniform mesh, or subgridding.* © 2008 Wiley Periodicals, Inc. Microwave Opt Technol Lett 50: 2335–2337, 2008; Published online in Wiley InterScience (www.interscience.wiley.com). DOI 10.1002/mop.23631

Key words: *FDTD; uniform mesh; nonuniform mesh; subgridding; impedance; dipole*

1. INTRODUCTION

FDTD method has become one of the major computational electromagnetic tools [1, 2]. Compared to method of moments (MoM) [3] and finite element method (FEM) [4], FDTD does not require a complicated mesh procedure and has more flexibility for the treatment of complex environment. A dipole antenna is formed by two quarter wavelength conductors placed back to back for a total half wavelength. Its radiation resistance at the input terminals can be expressed as:

$$R_{in} = 60Cin(2\pi) = 60[\ln(2\pi\gamma) - Ci(2\pi)]$$

$$= 120\int_0^{\frac{\pi}{2}} \frac{\mathrm{Cos}\left(\frac{\pi}{2}\cos(\vartheta)\right)^2}{\sin(\vartheta)} d\vartheta$$

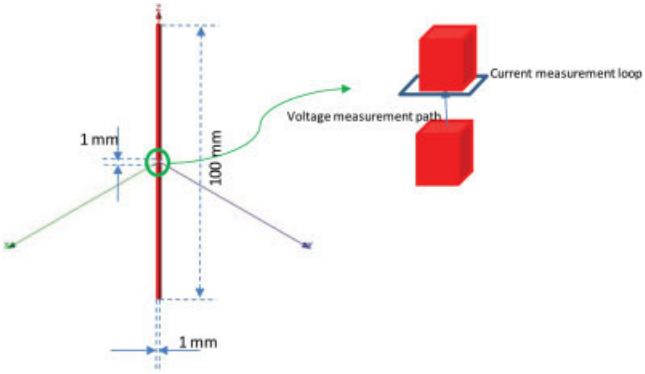

Figure 1 A half wavelength dipole. [Color figure can be viewed in the online issue, which is available at www.interscience.wiley.com]

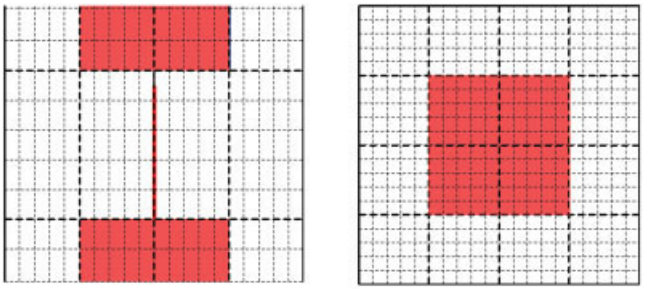

Figure 2 Mesh distribution in the first test case. [Color figure can be viewed in the online issue, which is available at www.interscience.wiley.com]

$$= 15\left[2\pi^2 - \frac{1}{3}\pi^4 + \frac{4}{135}\pi^6 - \frac{1}{630}\pi^8 + \frac{4}{70875}\pi^{10}\ldots - (-1)^n\frac{(2\pi)^{2n}}{n(2n)!}\right]$$

$$= 73.13\ \Omega$$

For a half wavelength dipole, its associated reactance (imaginary part) is $j42.5\Omega$. The actual resonant length of half wavelength dipole antenna is shorter than half wavelength. In this article, we use the FDTD code to calculate the resistance when the dipole is matched. Though the formula above looks like very simple, it is not easy for most EM simulation software to reach this value regardless of the shape of dipole cross section.

2. NUMERICAL EXPERIMENTS

A half wavelength dipole antenna is shown in Figure 1, whose cross section is a rectangular shape (1 mm × 1 mm). The dipole is excited by a voltage source and the feed gap size is 1 mm. The relative position of voltage and current measurement is also shown in Figure 1.

6-layer PML is used to truncate FDTD domain and 10 cells away from the dipole antenna. In the first test case, we choose $\Delta x = 0.1$ mm, $\Delta y = 0.1$ mm, and $\Delta z = 0.2$ mm, as shown in

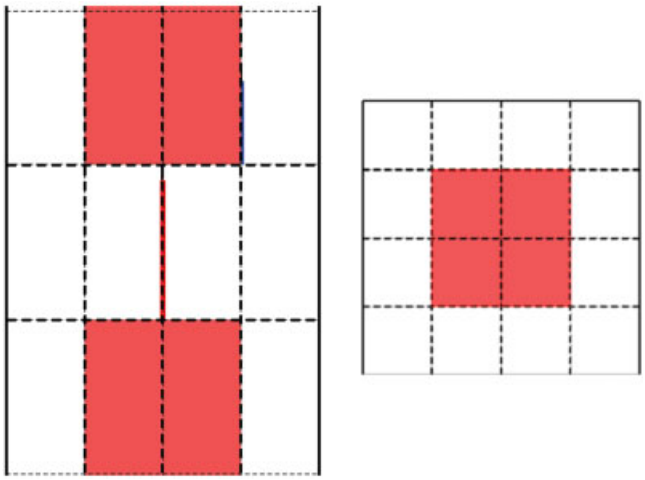

Figure 3 Mesh distribution in the second test case. [Color figure can be viewed in the online issue, which is available at www.interscience.wiley.com]

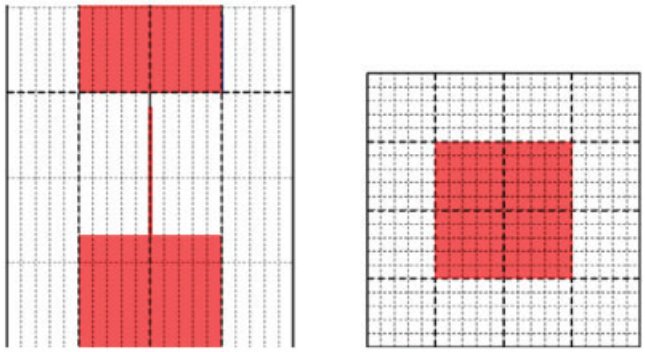

Figure 4 Mesh distribution in the third test case. [Color figure can be viewed in the online issue, which is available at www.interscience.wiley.com]

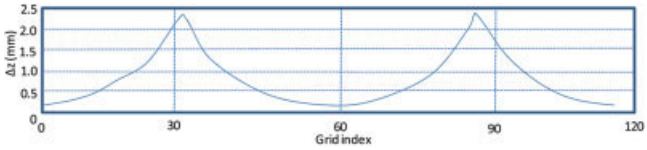

Figure 5 Mesh distribution in the z-direction. [Color figure can be viewed in the online issue, which is available at www.interscience.wiley.com]

Figure 2. In the second test case, we choose $\Delta x = 0.5$ mm, $\Delta y = 0.5$ mm, and $\Delta z = 1.0$ mm, as shown in Figure 3. And in the third test case, we choose $\Delta x = 0.1$ mm, $\Delta y = 0.1$ mm, and $\Delta z = 0.6$ mm, as shown in Figure 4. In both the first and second test cases, the resistance of half wavelength dipole is 73 Ω and the resonant frequency occurring at 1.325 GHz. The large ration of cell size in the vertical and horizontal directions will make the resistance of dipole antenna from 73 to 88 Ω.

To reduce the number of cells in the z-direction, we employ the nonuniform mesh distribution, namely, $\Delta x = 0.1$ mm, $\Delta y = 0.1$ mm, and $\Delta z_{min} = 0.2$ mm and $\Delta z_{max} = 2.3836$ mm, as shown in Figure 5. The number of cells in the z-direction is reduced from 500 in the first test case to 115. The resistance of half wavelength dipole is still 73 Ω and the resonant frequency occurring at 1.325 GHz.

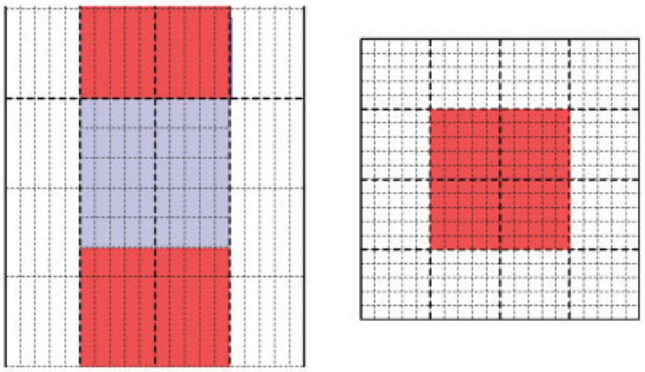

Figure 6 Subgridding mesh distribution in the z-direction. [Color figure can be viewed in the online issue, which is available at www.interscience.wiley.com]

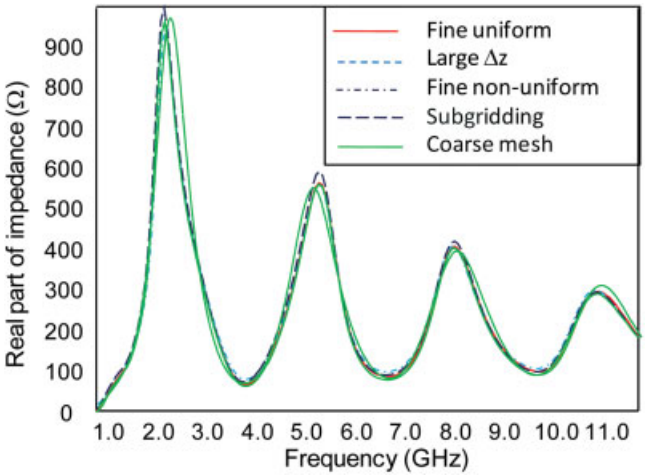

Figure 7 Real part of the input impedance of dipole antenna. [Color figure can be viewed in the online issue, which is available at www.interscience.wiley.com]

Now, we use a subgridding region in the feed area to simulate the dipole antenna again. We use the mesh distribution in the third test case, $\Delta x = 0.1$ mm, $\Delta y = 0.1$ mm, and $\Delta z = 0.6$ mm. The fine mesh inside the subgridding region is only in the z-direction using the ratio 3:1, as shown in Figure 6. The single precision is used both inside subgridding region and regular region outside. The resistance of half wavelength dipole is still 78 Ω and the resonant frequency occurring at 1.325 GHz.

The results simulated by using FDTD code [5] is summarized in the Figures 7 and 8. The FDTD project information is summarized in Table 1.

3. CONCLUSIONS

In this article, we use the FDTD method to calculate the impedance of half wavelength dipole antenna using different mesh types such as fine mesh, coarse mesh, nonuniform mesh, and subgridding. The result is in good agreement with analytic value.

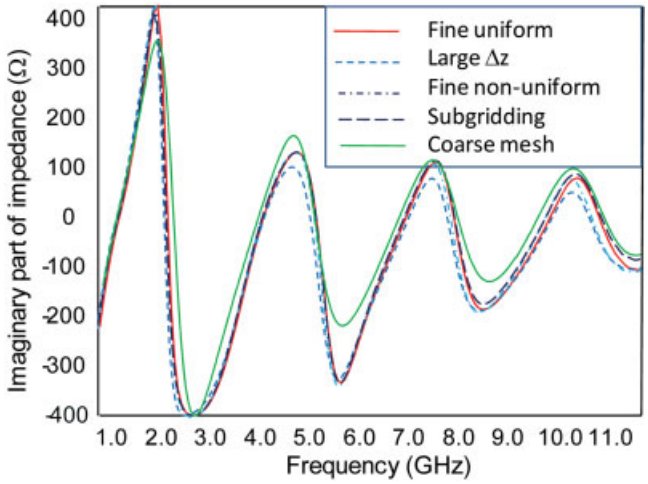

Figure 8 Imaginary part of the input impedance of dipole antenna. [Color figure can be viewed in the online issue, which is available at www.interscience.wiley.com]

TABLE 1 Summary of Input Impedance of Dipole Antenna

Mesh Types	Cell Size	No. of Cells	Time	Resonant Freq (GHz)	Impedance (Ω)
Fine mesh	$\Delta x = 0.1$ mm $\Delta y = 0.1$ mm $\Delta z = 0.2$ mm	$20 \times 20 \times 501$	0:3:12	1.38	73+j0
Large Δz	$\Delta x = 0.1$ mm $\Delta y = 0.1$ mm $\Delta z = 0.6$ mm	$20 \times 20 \times 168$	0:1:43	1.325	88+j0
Nonuniform	$\Delta x = 0.1$ mm $\Delta y = 0.1$ mm $\Delta z = 0.2$ mm	$20 \times 20 \times 115$	0:1:49	1.38	73+j0
Subgridding (Δzratio = 3:1)	$\Delta x = 0.1$ mm $\Delta y = 0.1$ mm $\Delta z = 0.6$ mm	$20 \times 20 \times 168$	0:6:59	1.375	78+j0
Coarse mesh	$\Delta x = 0.5$ mm $\Delta y = 0.5$ mm $\Delta z = 1.0$ mm	$4 \times 4 \times 101$	0:1:14	1.383	73+j0

ACKNOWLEDGMENTS

This research is partially sponsored by Communication University of China under 111 project.

REFERENCES

1. A. Taflove and S. Hagness, Computational electromagnetics: The finite-difference time-domain method, 3rd ed., Artech House, Norwood, 2005.
2. W. Yu, R. Mittra, T. Su, Y. Liu, and X. Yang, Parallel finite difference time domain method, Artech House, Norwood, 2006.
3. R. Harrington, Time-harmonic electromagnetic fields, IEEE Press, Piscataway, NJ, 2001.
4. J. Jin, The finite element method in electromagnetics, Wiley, New York, 2002.
5. GEMS software package, Computer and communication unlimited, State College, PA.

AN ALTERNATIVE ANALYTICAL REDUCTION SCHEME IN THE TIME-DOMAIN LAYERED FINITE ELEMENT REDUCTION RECOVERY METHOD FOR HIGH-FREQUENCY IC DESIGN

Houle Gan and Dan Jiao
School of Electrical and Computer Engineering, Purdue University, West Lafayette, IN 47907; Corresponding author: djiao@purdue.edu

Received 28 December 2007

ABSTRACT: *An alternative analytical reduction scheme was proposed in the time-domain layered finite element reduction recovery (LAFE-RR) method for the analysis of high-frequency integrated circuits. This alternative reduction scheme permits the use of general absorbing boundary conditions in the framework of a time-domain LAFE-RR method. In addition, it allows for an application of the LAFE-RR method to circuit problems in which the system matrices in multiple regions need to be reduced separately. Numerical and experimental results are given to demonstrate its validity.* © 2008 Wiley Periodicals, Inc. Microwave Opt Technol Lett 50: 2337–2341, 2008; Published online in Wiley InterScience (www.interscience.wiley.com). DOI 10.1002/mop.23630

Key words: *time-domain; finite element method; electromagnetic analysis; high frequency; integrated circuits*

1. INTRODUCTION

In the past three decades, driven by the continuous scaling of feature sizes and frequency, on-chip circuits have witnessed a series of transitions in modeling technology: from R (resistance)-based, RC (resistance-capacitance)-based, distributed RC-based, and RLC (resistance-inductance-capacitance)-based to transmission-line-based to full-wave electromagnetics-based analysis [1–8]. The increased level of integration across the entire electromagnetic spectrum necessitates the electromagnetics-based analysis even more. However, on-chip circuits present many modeling challenges [6] that are less pronounced in traditional full-wave applications such as antennas and waveguides. Among them, problem size is the No. 1 challenge. Ultra large-scale integration results in numerical problems of ultra large scale, requiring billions and billions of parameters to describe them accurately. In [7], to overcome the large problem size, a time-domain layered finite element reduction recovery (LAFE-RR) method was developed for high-frequency modeling and simulation of large-scale on-chip circuits. This method rigorously reduces the matrix of a multilayer system to that of a single-layer system, regardless of the original problem size. More importantly, the matrix reduction is achieved analytically, and hence the CPU and memory overheads are minimal. In addition, the reduction preserves the sparsity of the original system matrix. Numerical experiments have demonstrated four-orders-of-magnitude reduction in matrix factorization time. The superior performance applies to any arbitrarily shaped multilayer structure.

In this article, an alternative analytical reduction algorithm is proposed to further improve the capability of the LAFE-RR method. With this algorithm, the LAFE-RR method is generalized to support a variety of absorbing boundary conditions which cannot be supported by the original analytical reduction algorithm. In addition, it permits the application of the LAFE-RR method to circuit problems in which system reduction needs to be done separately for different regions.

2. FORMULATION

For the practical use of the LAFE-RR method, absorbing boundary conditions (ABCs) often need to be incorporated to truncate the computational domain. For example, in Figure 1, a circuit region of L layers is attached to two ABC regions, in which the outgoing waves are absorbed. The ABC region can be filled with air backed by a first-order absorbing boundary condition, or can be filled with